

Optimal reduction of an epidemic outbreak size via temporary quarantine

Eyal Atias* and Michael Assaf†

Racah Institute of Physics, Hebrew University of Jerusalem, Jerusalem 91904, Israel

Understanding the dynamics of an epidemic spread is crucial for effective control measures. During the COVID-19 pandemic, quarantines were implemented to minimize infections while mitigating social and economic impacts, raising the question of how to maximize quarantine efficiency. Previous research on periodic quarantines using the susceptible-infected-recovered (SIR) and similar models identified optimal duration for periodic quarantines. However, the question of the optimal *initiation* time for a single quarantine remains unanswered. Here, we use the SIR model in order to determine the optimal quarantine initiation time, by computing the optimal susceptible fraction at the onset of the quarantine, which minimizes the total outbreak size. Our analysis extends from a well-mixed scenario to strongly-heterogeneous social networks. We show that the optimal quarantine initiation time is closely related to the so-called “herd immunity” threshold, occurring at the onset of epidemic decline. Importantly, providing a methodology for identifying the optimal quarantine initiation time across different network structures, entails significant implications for epidemic control.

I. INTRODUCTION

Modeling and predicting the spread of pandemics has long intrigued researchers, leading to the development of various deterministic as well as stochastic epidemiological models [1–8]. One of the most fundamental models is the susceptible-infected-susceptible (SIS) model [5], which divides the population into two compartments: susceptibles (individuals who can get infected) and infected (individuals who can transmit the infection to susceptibles and eventually become susceptible again). This model is suitable for diseases such as influenza, or the common cold, with relatively short-term immunity such that individuals can be reinfected after being recovered.

A more realistic model which is widely used to characterize the spread of epidemics is the susceptible-infected-recovered (SIR) model, which complements the SIS model with a third *recovered* compartment [8]. Here, the underlying assumption is long-term immunity such that recovered individuals do not get reinfected immediately. Naturally, the SIR can be generalized, e.g., by including the possibility of reinfection, or adding an *exposed* phase prior to infection, to account for an incubation period of the disease [8]. The SIR model and its generalizations are amply used to describe the dynamics of a wide variety of diseases such as measles, chickenpox, rubella, smallpox, polio, and severe acute respiratory syndrome (SARS), including the recent COVID-19 pandemic [9, 10].

One of the most important factors that determine the disease dynamics is the topology of the population network, namely, the structure of the social contacts within the population. The simplest form of topology is the so-called “well-mixed” setting, where each individual is equally connected to all other individuals [1, 5, 11–13]. Indeed, this setting holds, e.g., when the population is confined to a relatively small area, and each individual

can interact with all others. Yet, a more realistic scenario includes a nontrivial population network, where each individual is represented by a node, and has a certain *degree*, which determines the number of contacts, or edges, through which infection can spread. Here, the network is often characterized by a degree distribution, providing information about the likelihood of having a specific number of connections. For generic degree distributions these networks are called *heterogeneous*, providing a clear departure from classic compartmental models, such that key quantities including epidemic and herd-immunity thresholds, expected outbreak size, and disease lifetime, may dramatically vary, see e.g., [14–19]. Notable examples for such population networks are homogeneous networks, in which each node has an equal degree, Erdős-Rényi networks [20] with a Poisson degree distribution (for large networks), gamma-distributed [21] and power-law [22, 23] networks. Notably, the well-mixed setting is a particular example of a homogeneous network where the degree of each node equals the population size.

While the well-mixed scenario has been extensively analyzed, and both the expected outbreak size, as well as its distribution have been rigorously found [1, 5, 10–13, 24–30], dealing with the SIR model on heterogeneous networks is more intricate. Here, most works dealing with generic networks have focused on the deterministic (or mean-field) dynamics, while keeping the infection and recovery rates constant [31–35]. Recently, a generalized SIR model with time-fluctuating infection and recovery rates has been studied, in a well-mixed setting [30]. Yet, a systematic analysis of the SIR model on heterogeneous population networks with explicitly time-dependent rates, has not been carried out so far.

In this work we focus on the SIR model on generic population networks, and study how the mean-field dynamics, and in particular, the expected outbreak size, are affected when a temporary quarantine is introduced during the epidemic wave. The quarantine is implemented by abruptly decreasing the infection rate by a given factor at some given time and for a prescribed duration, due to intervention measures such as increased seclusion [36].

* eyal.atias1@mail.huji.ac.il

† michael.assaf@mail.huji.ac.il

Subsequently, the quarantine is lifted and the infection rate goes back to its pre-quarantine value.

The primary aim of implementing quarantine measures is to mitigate the spread of infection and thus control the epidemic. Here, a key question is how to make the quarantine most efficient, given that its duration and magnitude are fixed. Recently there have been some works dealing with quarantines and ways to optimize them. In Ref. [37] the authors have dealt with a generalized SIR model and studied how the overall cost of a quarantine can be minimized. In [36, 38] periodic quarantines were studied: in Ref. [38] the optimal quarantine duration was computed using a generalized SIR model, whereas in Ref. [36] the authors have studied an alternating quarantine (each time on half of the population) and how it can be optimally synchronized with the disease lifetime.

We here study a different angle and ask the following question: given a quarantine of prescribed duration and magnitude, is there an optimal *initiation* time of the quarantine, such that the expected final outbreak size is minimized? Remarkably, our results reveal that indeed there exists an optimal quarantine onset, which gives rise to a minimization of the overall expected number of infected during the epidemic wave. Notably, since the fraction of susceptibles is a monotone decreasing function of time, the optimal initiation time of the quarantine can be converted into an optimal susceptible fraction. Once this optimal fraction is reached, one can strategically time the initiation of quarantine measures, holding significant implications for managing future pandemics.

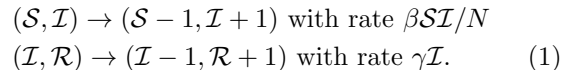
This rest of the paper is organized as follows. Section II introduces the theoretical model and provides a methodology for determining the optimal moment to initiate quarantine, for a variety of network topologies. Section III details the results for the different networks and our numerical algorithm used to validate the theoretical findings. Finally, Sec. IV presents our conclusions, and offers an explanation and interpretation of the results.

II. THEORETICAL FORMULATION

A. Well-mixed setting

In the SIR model, the population is comprised of three compartments: \mathcal{S} , \mathcal{I} and \mathcal{R} , denoting the numbers of susceptibles, infected and recovered in the population, respectively. In the absence of demography, the total population size is conserved: $\mathcal{S} + \mathcal{I} + \mathcal{R} = N$, where N is the total size of the population network, and we assume throughout this work that $N \gg 1$. In a well-mixed setting, the probability per unit time that the number of susceptibles decreases by one and the number of infected increases by one is $\beta\mathcal{S}\mathcal{I}/N$, where β is the infection rate per individual. Similarly, the probability per unit time that the number of infected decreases by one is $\gamma\mathcal{I}$, where γ is the recovery rate per individual. Combining both processes results in a discrete-state system with the fol-

lowing stochastic reactions:



For simplicity, we introduce the fractions of susceptibles $S = \mathcal{S}/N$, infected $I = \mathcal{I}/N$, and recovered $R = \mathcal{R}/N$. Denoting the basic reproduction number $R_0 = \beta/\gamma$, rescaling time $t \rightarrow \gamma t$, and assuming a well-mixed setting of a fully-connected population of $N \gg 1$ individuals, the deterministic rate equations read:

$$\dot{S} = -\mathfrak{R}(t)SI, \quad \dot{I} = \mathfrak{R}(t)SI - I, \quad \dot{R} = I. \quad (2)$$

These equations require an initial condition: we assume an initial fractions of I_0 infected, and $S(t=0) = 1 - I_0$ susceptibles. Our aim is to determine the *optimal* susceptible fraction, S_{opt} , at which the quarantine is initiated, such that the final outbreak size is minimized.

As the epidemic progresses, a quarantine is initiated at time $t_0 > 0$, when the fraction of susceptibles right *before* the quarantine is denoted by $S_b \equiv S(t=t_0)$. At this point, the infection rate drops from β to $\xi\beta$, with $0 \leq \xi < 1$, for a prescribed duration Δt . At $t = t_0 + \Delta t$ the infection rate returns to its pre-quarantine value, until the epidemic wave is over. At the deterministic level, the dynamics satisfy Eq. (2), with an explicitly time-dependent basic reproduction number \mathfrak{R} :

$$\mathfrak{R}(t) = \begin{cases} R_0 & t < t_0 \text{ or } t > t_0 + \Delta t \\ R_0\xi & t_0 < t < t_0 + \Delta t, \end{cases} \quad (3)$$

where R_0 is the basic reproduction number in the pre- and post-quarantine stages.

We now determine the final outbreak fraction of the epidemic, denoted as $R_\infty = R(t \rightarrow \infty)$, as a function of I_0 , ξ , S_b , R_0 , and Δt . Following Ref. [23], we define a new time scale τ such that $\dot{\tau} = \mathfrak{R}I$. This readily yields:

$$S(\tau) = (1 - I_0)e^{-\tau}. \quad (4)$$

While $S(\tau)$ takes a rather simple form, $I(\tau)$ has to be determined in three separate regimes: before, during, and after the quarantine, since $\mathfrak{R} = \mathfrak{R}(t)$. Demanding continuity of $I(\tau)$, after some algebra we find:

$$\begin{aligned} I(\tau) &= (I_0 - 1)e^{-\tau} + f(\tau), \\ f(\tau) &= \begin{cases} -\frac{\tau}{R_0} + 1 & \tau < \tau_0, \\ -\frac{\tau}{R_0\xi} + 1 + \frac{\tau_0}{R_0} \left(\frac{1}{\xi} - 1\right) & \tau_0 < \tau < \tau_0 + \Delta\tau, \\ -\frac{\tau}{R_0} + 1 + \frac{\Delta\tau}{R_0} \left(1 - \frac{1}{\xi}\right) & \tau > \tau_0 + \Delta\tau. \end{cases} \end{aligned} \quad (5)$$

Here τ_0 is found from $S(\tau)$ and reads $\tau_0 = \ln[(1 - I_0)/S_b]$. In addition, $\Delta\tau$ can be determined using the equation for $\dot{\tau} = \mathfrak{R}I = \xi R_0 I$ during the quarantine, leading to:

$$\int_{\tau_0}^{\tau_0 + \Delta\tau} \frac{d\tau'}{1 + \frac{\tau_0}{R_0} (\xi^{-1} - 1) - (1 - I_0)e^{-\tau'} - \frac{\tau'}{R_0\xi}} = R_0\xi\Delta t. \quad (6)$$

This allows to compute R_∞ by using the fact that $\dot{R} = I$ and $\dot{\tau} = \mathfrak{R}(t)\dot{R}$, which yields $R(\tau) = \tau/\mathfrak{R}(t) + C$, where C is a constant. Demanding continuity of $R(\tau)$, we find:

$$R(\tau) = \begin{cases} \frac{1}{R_0}\tau & \tau < \tau_0, \\ \frac{1}{R_0\xi}\tau + \frac{\tau_0}{R_0}\left(1 - \frac{1}{\xi}\right) & \tau_0 < \tau < \tau_0 + \Delta\tau, \\ \frac{1}{R_0}\tau + \frac{\Delta\tau}{R_0}\left(\frac{1}{\xi} - 1\right) & \tau > \tau_0 + \Delta\tau. \end{cases} \quad (7)$$

Using the last regime, we obtain $\tau_\infty = R_0 R_\infty + (1 - \xi^{-1})\Delta\tau$, which, with $S_\infty = (1 - I_0)e^{-\tau_\infty}$ and $R_\infty = 1 - S_\infty$, yields a closed-form equation for R_∞ . The solution satisfies:

$$R_\infty = 1 + \frac{1}{R_0}W_0\left[-R_0e^{-R_0}(1 - I_0)e^{(\xi^{-1}-1)\Delta\tau}\right], \quad (8)$$

where $W_0(x)$ is the main branch of Lambert's W function, and $\Delta\tau$ is given by Eq. (6), with τ_0 given right below Eq. (5). Note that, in the absence of a quarantine (i.e., $\xi = 1$), we arrive at the known results [23]:

$$I(\tau) = (I_0 - 1)e^{-\tau} - \frac{\tau}{R_0} + 1, \quad R(\tau) = \frac{1}{R_0}\tau$$

$$R_\infty = 1 + \frac{1}{R_0}W_0\left[-R_0e^{-R_0}(1 - I_0)\right]. \quad (9)$$

In Fig. 1 we illustrate an example of an epidemic outbreak. One can see the fractions S , I and R versus time (left) and τ (right), where the latter depends on time nontrivially. Using the fact that $\dot{\tau} = \mathfrak{R}(t)I$, we find:

$$\int_0^\tau \frac{d\tau'}{I(\tau')} = \int_0^t \mathfrak{R}(t)dt, \quad (10)$$

where $I(\tau)$ and $\mathfrak{R}(t)$ are given by Eqs. (3) and (5). In this figure, a quarantine is introduced when the fraction of susceptibles is 70%, i.e. $S_b = 0.7$, such that the infection rate during the quarantine drops to 40% its pre-quarantine value. As expected, a discontinuity in the derivatives of $S(t)$ and $I(t)$ is displayed, at the start and end of the quarantine. Note that, in the right panel of Fig. 1, the fractions are plotted versus $\tau(t)$, which is proportional to $R(t)$, hence the linear piecewise behavior of $R(\tau)$. In contrast, $S(\tau)$ remains smooth as function of τ in all three regimes [see Eq. (4)].

To find the optimal susceptible fraction at the quarantine onset, S_{opt} , we differentiate Eq. (8) with respect to S_b . Since only $\Delta\tau$ depends on S_b in Eq. (8) via Eq. (6) (as τ_0 depends on S_b), dR_∞/dS_b reads:

$$\frac{dR_\infty}{dS_b} = \frac{1}{R_0} \frac{W_0(x)}{1 + W_0(x)} \frac{d\Delta\tau}{dS_b}, \quad (11)$$

where $x = -R_0e^{-R_0}(1 - I_0)e^{(\xi^{-1}-1)\Delta\tau}$. Equating (11) to zero allows to determine S_{opt} that minimizes R_∞ . To this end, as $W_0(x \neq 0) \neq 0$, it is sufficient to demand that $\Delta\tau'(S_b) = 0$, where $\Delta\tau(S_b)$ is given by Eq. (6).

In general, for an arbitrary quarantine duration, com-

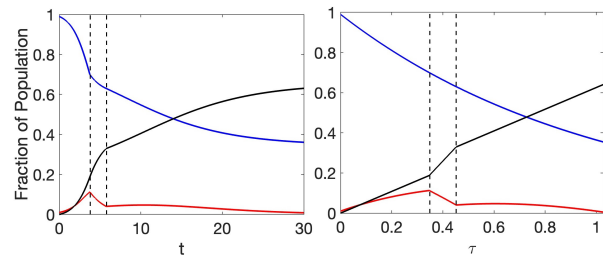


FIG. 1. SIR dynamics in the presence of a temporary quarantine. Shown are fractions of susceptibles (blue lines), infected (red lines) and recovered (black lines) versus time (left) and τ (right). Here $R_0 = 1.85$, $\xi = 0.4$, $S_b = 0.7$, and $\Delta t = 2$. Dashed vertical lines mark the quarantine boundaries.

puting this derivative can only be done numerically. Yet, for $\Delta t \ll 1$, we can approximate the integral in Eq. (6) by Taylor-expanding the result at $\Delta\tau \ll 1$ [39]. Since the denominator of (6) equals $I(\tau')$, for $\Delta\tau \ll 1$ we have:

$$\int_{\tau_0}^{\tau_0+\Delta\tau} \frac{d\tau'}{I(\tau')} \simeq \frac{\Delta\tau}{I(\tau_0)} - \frac{(\Delta\tau)^2}{2} \frac{I'(\tau_0)}{I(\tau_0)^2}. \quad (12)$$

Plugging this approximation into Eq. (6) allows us to find $\Delta\tau$ as function of Δt and S_b , and subsequently find $d\Delta\tau/dS_b$. Equating this derivative to zero, and solving perturbatively with respect to $\Delta t \ll 1$, we are able to find the leading- and subleading-order terms in S_{opt} order by order in $\Delta t \ll 1$ [40]. The result is

$$S_{\text{opt}} \simeq \frac{1}{R_0} + \left(\frac{R_0 - \ln R_0 - 1}{2R_0}\right) \xi \Delta t. \quad (13)$$

Importantly, in the limit $\Delta t \rightarrow 0$, the optimal susceptible fraction at the quarantine onset coincides with the herd immunity (HDI) threshold S_{hdi} , which equals $1/R_0$ for fully-connected networks in the absence of quarantine measures. This threshold represents the point at which the infected population reaches its peak and starts declining. Our result indicates that the longer the quarantine duration is, the earlier it has to be initiated, before the HDI threshold is reached, in order to minimize R_∞ .

B. Heterogeneous Networks

We now determine S_{opt} for heterogeneous population networks. Here, unlike a well-mixed population, each individual is connected according to a prescribed degree distribution p_k , denoting the probability for a node in the network to have k connections, such that $\sum_k p_k = 1$.

When dealing with population networks it is convenient to define the infection rate β per contact (rather than per individual), whereas γ still denotes the recovery rate per individual, and time is measured in units of γ^{-1} . Denoting $k_0 = \sum_k k p_k$ and $\sigma^2 = \sum_k k^2 p_k - k_0^2$ as the distribution's mean and variance, the basic reproduc-

tion number R_0 (in the absence of a quarantine) satisfies:

$$R_0 = \beta/\beta_c, \quad \beta_c = k_0/(k_0^2 + \sigma^2 - 2). \quad (14)$$

Here, β_c is the critical infection rate below which the epidemic dies out instantly [11, 41, 42]. For simplicity we will focus on networks with $k_0 \gg 1$ such that $\beta_c \simeq k_0/(k_0^2 + \sigma^2)$. Notably, when $\sigma = 0$ and $k_0 = N$, $\beta_c = 1/N$ and $R_0 = N\beta$, as expected in the well-mixed case.

To illustrate the dependence of R_∞ on S_b and to show the existence of an optimal S_b , we plot in Fig. 2 heatmaps depicting R_∞ as function of S_b and R_0 (a,c) and Δt (b,d), for Poisson and gamma population networks, see below. The heatmaps clearly demonstrate the existence of S_{opt} that minimizes the final outbreak fraction R_∞ , for a wide range of R_0 values and quarantine durations Δt . In fact, S_{opt} grows (almost linearly) as function of Δt , see below, indicating that the quarantine should be initiated earlier as Δt is increased. Conversely, S_{opt} decreases as R_0 increases, suggesting that the quarantine should be delayed as the basic reproduction number grows.

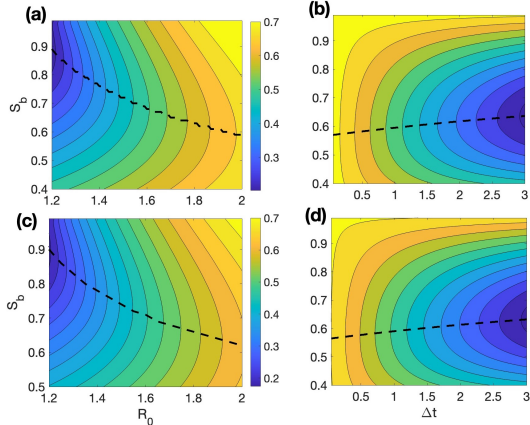


FIG. 2. Heatmaps of R_∞ for two different population networks. Shown is R_∞ versus S_b and R_0 (a,c) and S_b and Δt (b,d). Upper (a,b) and lower (c,d) panels show results for a Poisson and gamma network, respectively. In all panels $k_0 = 50$ and $\xi = 0.5$. In (a,c) $\Delta t = 2$, while in (b,d) $R_0 = 1.85$. In (c,d) the gamma network has a COV of $\epsilon = 0.27$, see text. The black dashed lines denote S_{opt} .

To study the dependence of R_∞ on S_b we adopt the approach of Ref. [35]. We denote by $\theta(t)$ the fraction of edges that have not yet transmitted the infection up to time t . This definition is equivalent to the probability that a node of degree 1 is still susceptible at time t [35]. Thus, the probability of an individual node with k contacts to remain susceptible at time t is given by θ^k . As a result, the fraction of susceptibles at time t is given by

$$S(t) = \Psi(\theta(t)) = \sum_{k=1}^{\infty} p_k \theta(t)^k, \quad (15)$$

where $\Psi(\theta)$ is the probability generating function of the degree distribution [35]. Our aim is to find $\theta(t)$, and subsequently θ_∞ , such that $R_\infty = 1 - \sum_{k=1}^{\infty} p_k \theta_\infty^k$. Following

the methodology in [35] the dynamics of $\theta(t)$ satisfies:

$$\dot{\theta} = -\beta(t)\phi, \quad \dot{\phi} = -[1 + \beta(t) - (\beta(t)/k_0)\Psi''(\theta)]\phi, \quad (16)$$

where ϕ denotes the fraction of edges that have not yet transmitted infection, and have an infected base node. Combining Eqs. (16), the dynamics satisfy:

$$\dot{\phi} = [1 + \beta(t)^{-1} - (1/k_0)\Psi''(\theta)]\dot{\theta}. \quad (17)$$

Given that the quarantine starts at time $t_0 > 0$ and ends at time $t_0 + \Delta t$, Eq. (17) needs to be solved in three regimes: (i) pre-quarantine $0 \leq t \leq t_0$ with an infection rate β ; (ii) during the quarantine $t_0 \leq t \leq t_0 + \Delta t$ with an infection rate $\beta\xi$; and (iii) post-quarantine $t > t_0 + \Delta t$ with an infection rate β . Naturally, the integration constants must be such that $\theta(t)$ is continuous at all times.

At this point we note that in addition to $\theta(t)$ being a continuous function of time, $\phi(t)$ must be continuous as well. Suppose ϕ has a finite discontinuity at $t = t_0$ and at $t = t_0 + \Delta t$. Since $\beta(t)$ has a finite discontinuity at those times as well, $\dot{\phi}$ will also have a finite discontinuity exactly at those times, as $\dot{\phi}$ is proportional to ϕ , and $\Psi''(\theta)$ is a continuous function of θ , see Eq. (15). Yet, if ϕ has a finite discontinuity, its integral with respect to time, θ , must be continuous at those times, in contradiction to our initial assumption. Hence, ϕ is continuous.

Once we have established that both θ and ϕ are continuous functions of time, despite the discontinuity in the infection rate $\beta(t)$, we can integrate Eq. (17) between $t = 0$ and $t = t_0$, between $t = t_0$ and $t = t_0 + \Delta t$, and between $t = t_0 + \Delta t$ and $t = \infty$. This results in:

$$\begin{aligned} \phi_b - \phi_0 &= (1 + \beta^{-1})(\theta_b - \theta_0) - k_0^{-1} [\Psi'(\theta_b) - \Psi'(\theta_0)], \\ \phi_a - \phi_b &= (1 + (\beta\xi)^{-1})(\theta_a - \theta_b) - k_0^{-1} [\Psi'(\theta_a) - \Psi'(\theta_b)], \\ \phi_\infty - \phi_a &= (1 + \beta^{-1})(\theta_\infty - \theta_a) - k_0^{-1} [\Psi'(\theta_\infty) - \Psi'(\theta_a)], \end{aligned} \quad (18)$$

where $\theta_0 = \theta(t=0) \simeq 1$, $\theta_b = \theta(t_0)$ and $\theta_a = \theta(t_0 + \Delta t)$ are the values of θ right before and right after the quarantine, respectively, and $\theta_\infty = \theta(t \rightarrow \infty)$ (and the same notation applies to ϕ). Summing up these equations, and noting that $\dot{\theta}_0 \simeq \dot{\theta}_\infty \simeq 0$ and thus, $\phi_0 \simeq \phi_\infty \simeq 0$, and that $\Psi'(\theta_0) \simeq \Psi'(1) = k_0$, we arrive at an equation for θ_∞ :

$$\left(1 + \frac{1}{\beta}\right)(\theta_\infty - 1) + \frac{\Delta\theta}{\beta} \left(1 - \frac{1}{\xi}\right) - \frac{\Psi'(\theta_\infty)}{k_0} + 1 = 0, \quad (19)$$

where $\Delta\theta(\Delta t, S_b) \equiv \theta_b - \theta_a$. To find S_{opt} we differentiate Eq. (19) with respect to S_b which yields:

$$\frac{d\theta_\infty}{dS_b} = \frac{k_0(1 - \xi)}{\xi[k_0 + k_0\beta - \beta\Psi''(\theta_\infty)]} \frac{d\Delta\theta}{d\theta_b}. \quad (20)$$

Thus, to minimize R_∞ (maximize θ_∞), we equate $\Delta\theta'(\theta_b) = 0$ and find θ_{opt} —the optimal value of θ_b . This allows finding S_{opt} [Eq. (15)], which minimizes R_∞ .

Note that, in order to find the optimal susceptible fraction at the onset of quarantine, it is sufficient to numerically

ically solve the rate equation during the quarantine. Indeed, starting from Eq. (17) and differentiating the first of Eqs. (16) with respect to time (during the quarantine), we arrive at a second-order differential equation for θ . Integrating this equation between $t = t_0$ and $t = t_0 + \Delta t$, and noting that $\theta(t)$ is continuous at all times, we arrive at the following first-order equation for θ :

$$\dot{\theta} = -(1 + \beta\xi)\theta(t) + \xi + \theta_b(1 - \xi) + (\beta\xi/k_0)\Psi'[\theta(t)], \quad (21)$$

which is numerically solved with the initial condition $\theta(t_0) = \theta_b$. The solution of this equation allows finding $\Delta\theta$ as function of θ_b , where the latter is arbitrary. Differentiating $\Delta\theta$ with respect to θ_b and equating to zero yields θ_{opt} and the optimal susceptible fraction.

While we have outlined a complete recipe of finding the optimal fraction of susceptibles that minimizes R_∞ , explicit analytical progress can be made in the limit of short quarantine, $\Delta t \ll 1$, as was done in the well-mixed topology. To do so, we take Eq. (21), estimate it at time $t = t_0 + \Delta t/2$, and use the approximations $\dot{\theta} \simeq -\Delta\theta/\Delta t$ and $\theta(t) \approx (\theta_b + \theta_a)/2 = \theta_b - \Delta\theta/2$. This yields an approximate equation for $\Delta\theta$, valid at $\Delta t \ll 1$:

$$\frac{\Delta\theta}{\Delta t} \simeq \theta_b\xi(1 + \beta) - \frac{\Delta\theta}{2}(1 + \beta\xi) - \xi - \frac{\beta\xi}{k_0}\Psi'\left(\theta_b - \frac{\Delta\theta}{2}\right). \quad (22)$$

Taylor-expanding $\Psi'(\theta_b - \Delta\theta/2) \approx \Psi'(\theta_b) - \Psi''(\theta_b)\Delta\theta/2$, we can thus write $\Delta\theta$ in terms of Δt (up to second order):

$$\Delta\theta = \Delta\theta(\theta_b) \simeq \left[\theta_b(\beta + 1) - 1 - \frac{\beta\Psi'(\theta_b)}{k_0} \right] \xi \Delta t \\ \times \left[1 - \left(1 + \beta\xi - \frac{\beta\xi\Psi''(\theta_b)}{k_0} \right) \frac{\Delta t}{2} \right]. \quad (23)$$

To find θ_{opt} [see Eq. (20)], we need to differentiate this equation with respect to θ_b and equate to zero, yielding:

$$0 = \frac{d\Delta\theta}{d\theta_b} = [(\beta + 1)k_0 - \beta\Psi''(\theta_b)] \frac{\xi\Delta t}{k_0} \\ + \{\beta\xi[k_0(-1 + \theta_b + \beta\theta_b) - \beta\Psi'(\theta_b)]\Psi'''(\theta_b) \\ - [((\beta + 1)k_0 - \beta\Psi''(\theta_b))(k_0 + k_0\beta\xi - \beta\xi\Psi''(\theta_b))]\} \frac{\xi\Delta t^2}{2k_0^2}.$$

We now solve this equation perturbatively, by plugging $\theta_b = \theta_{\text{opt}} \simeq \theta_{\text{opt}}^{(0)} + \theta_{\text{opt}}^{(1)}\Delta t$ into (24). In the leading-order in $\Delta t \ll 1$, we arrive at an implicit equation for $\theta_{\text{opt}}^{(0)}$:

$$\Psi''\left(\theta_{\text{opt}}^{(0)}\right) = (\beta + 1)k_0/\beta. \quad (25)$$

The next-order correction, $\theta_{\text{opt}}^{(1)}$, is found by plugging $\theta_{\text{opt}}^{(0)}$ in the $\mathcal{O}(\Delta t^2)$ term in Eq. (24). This yields:

$$\theta_{\text{opt}}^{(1)} = \frac{\xi}{2} \left[-1 + (1 + \beta)\theta_{\text{opt}}^{(0)} - (\beta/k_0)\Psi'(\theta_{\text{opt}}^{(0)}) \right]. \quad (26)$$

Having found $\theta_{\text{opt}} \simeq \theta_{\text{opt}}^{(0)} + \theta_{\text{opt}}^{(1)}\Delta t$, the optimal fraction of susceptibles at the onset of quarantine reads

$$S_{\text{opt}} \simeq \Psi\left(\theta_{\text{opt}}^{(0)}\right) + \Psi'\left(\theta_{\text{opt}}^{(0)}\right)\theta_{\text{opt}}^{(1)}\Delta t. \quad (27)$$

We will now apply these results to three examples of networks: homogeneous, Poisson, and gamma networks.

1. Homogeneous Network

In a homogeneous network each node has an equal number of k_0 neighbors, and the degree distribution satisfies $p_k = \delta_{k,k_0}$. Thus $\Psi(\theta)$ [Eq. (15)] becomes

$$\Psi(\theta) = \theta^{k_0}, \quad (28)$$

or alternatively, $\theta = S^{1/k_0}$. As a result, in the general case one can solve Eq. (21) and find the optimal fraction of susceptibles S_{opt} , by numerically differentiating $\Delta\theta(\Delta t, S_b) = S_b^{1/k_0} - S_a^{1/k_0}$ with respect to θ_b .

In the limit of short quarantine times, $\Delta t \ll 1$, we use Eqs. (25) and (26) to find $\theta_{\text{opt}}^{(0)}$ and $\theta_{\text{opt}}^{(1)}$. Substituting these expressions into Eq. (27) and taking the limit of $k_0 \gg 1$, we arrive at:

$$S_{\text{opt}} \simeq \frac{1}{R_0} \left(1 + \frac{1 + R_0 - 2 \ln R_0}{k_0} \right) + \left(\frac{R_0 - \ln R_0 - 1}{2R_0} \right) \xi \Delta t, \quad (29)$$

where we have omitted $\mathcal{O}(k_0^{-1})$ terms in the $\mathcal{O}(\Delta t)$ term. Note that, in the limit $k_0 \rightarrow \infty$ we restore the result for the optimal fraction of susceptibles at the onset of quarantine, for a well-mixed network.

2. Poisson Network

In a Poisson network (also known as the Erdős-Rényi network [20] for large networks), the degree distribution follows a Poisson distribution $p_k = (1/k!)k_0^k e^{-k_0}$, which has a mean degree of k_0 . Here, $\Psi(\theta)$ [Eq. (15)] becomes

$$\Psi(\theta) = e^{-k_0}(e^{k_0\theta} - 1), \quad (30)$$

or alternatively, $\theta = (1/k_0)\ln(e^{k_0}S + 1)$. As a result, in the general case one can solve Eq. (21) and find S_{opt} by numerically differentiating $\Delta\theta(\Delta t, S_b) = (1/k_0)\ln[(S_b + e^{-k_0})/(S_a + e^{-k_0})]$ with respect to θ_b .

In the limit of short quarantine times, $\Delta t \ll 1$, we use Eqs. (25) and (26) to find $\theta_{\text{opt}}^{(0)}$ and $\theta_{\text{opt}}^{(1)}$. Substituting these into Eq. (27) and taking the limit of $k_0 \gg 1$, yields:

$$S_{\text{opt}} \simeq \frac{1}{R_0} \left(1 + \frac{1 + R_0}{k_0} \right) + \left(\frac{R_0 - \ln R_0 - 1}{2R_0} \right) \xi \Delta t, \quad (31)$$

where we have neglected the term e^{-k_0} in the zeroth-order in Δt , as this term is exponentially small when

$k_0 \gg 1$. In addition, as done in the homogeneous network case, we have omitted $\mathcal{O}(k_0^{-1})$ terms in the $\mathcal{O}(\Delta t)$ term. The fact that the Poisson distribution has a relative width scaling as $k_0^{-1/2} \ll 1$, gives rise to the resemblance to the homogeneous case. Finally, in the limit $k_0 \rightarrow \infty$, we again restore the well-mixed result for S_{opt} .

3. Gamma distribution

We now consider a more general class of networks with two parameters such that the mean and standard deviation can be controlled separately. As a prototypical example we consider the gamma distribution, which is used in this realm to describe population heterogeneity [23, 42]. In this case, the degree distribution satisfies

$$p_k = \frac{k^{1/\epsilon^2 - 1} e^{-k/(k_0 \epsilon^2)}}{\Gamma(1/\epsilon^2)(k_0 \epsilon^2)^{1/\epsilon^2}}. \quad (32)$$

Here, we have adjusted the shape and scale parameters such that the mean and variance respectively are k_0 and $\sigma^2 = \epsilon^2 k_0^2$, while $\epsilon = \sigma/k_0$ is the distribution's coefficient of variation. As a result, $\Psi(\theta)$ [Eq. (15)] becomes

$$\Psi(\theta) = [1 - k_0 \epsilon^2 \ln(\theta)]^{-1/\epsilon^2}, \quad (33)$$

or alternatively, $\theta = \exp[(1 - S^{-\epsilon^2})/(k_0 \epsilon^2)]$. As a result, in the general case one can solve Eq. (21) and find the optimal fraction of susceptibles by numerically differentiating $\Delta\theta(\Delta t, S_b)$ with respect to θ_b .

Unfortunately, the limit of short quarantine duration $\Delta t \ll 1$, is not amenable in the general case here, as Eq. (25) cannot be solved analytically. Yet, we can solve the short-duration case numerically, see below. Nevertheless, analytical progress can be made in the limit of small coefficient of variation, $\epsilon \ll 1$, or $\sigma \ll k_0$, see below.

4. General network

Here we formulate an expression for the optimal fraction of susceptibles S_{opt} , which minimizes the expected outbreak size. We do so for generic networks, with an arbitrary degree distribution p_k , but under three assumptions: (i) the distribution's mean is large $k_0 \gg 1$, (ii) the coefficient of variation is small, $\epsilon \ll 1$, and (iii) the duration of the quarantine is short, $\Delta t \ll 1$.

Under these assumptions we begin by computing the subleading $\mathcal{O}(\Delta t)$ correction to S_{opt} , see Eqs. (26) and (27). To do so, we use a very crude approximation, assuming that the distribution is a delta function peaked at $k = k_0$, namely $p_k = \delta_{k,k_0}$, as in the homogeneous case. As a result, we have $\Psi(\theta) \sim \theta^{k_0}$. Plugging this result into Eq. (25) and putting $\beta \simeq R_0/k_0$ (valid when $\sigma \ll k_0$), we find $\theta_{\text{opt}}^{(0)} \simeq R_0^{-1}(1 + \alpha/k_0)$, where $\alpha \ll k_0$ is a constant depending on R_0 and the higher cen-

tral moments of the degree distribution. Consequently, we plug this result into Eq. (26) and use the fact that $\Psi'(\theta) \sim k_0 \theta^{k_0 - 1}$. In the leading order in $k_0 \gg 1$, this yields $\theta_{\text{opt}}^{(1)} \simeq \xi(R_0 - \ln R_0 - 1)/(2k_0)$. As a result, the optimal susceptible fraction [Eq. (27)] becomes:

$$S_{\text{opt}} \approx \Psi(\theta_{\text{opt}}^{(0)}) + \left(\frac{R_0 - \ln R_0 - 1}{2R_0}\right) \xi \Delta t, \quad (34)$$

where the leading-order term given by Eq. (15) is not yet calculated. It is implicitly given by Eq. (25) and we now show how this term can also be approximately found by using a slightly more subtle approximation.

To compute the leading-order term, it is not sufficient to assume that the distribution is a delta function around $k_0 \gg 1$. Rather, we assume that it is a narrow distribution with a standard deviation $\sigma \ll k_0$. For such networks, $\Psi(\theta)$ can in principle be evaluated using a saddle point approximation. Indeed, in this regime we can approximate $\Psi(\theta)$ given by Eq. (15) as an integral and evaluate it via the saddle point method:

$$\Psi(\theta) \simeq \int_0^\infty p(k) \theta^k dk \simeq A p(k_0) \theta^{k_0}, \quad (35)$$

where we have assumed that the saddle point k^* approximately equals k_0 , and A is a prefactor depending on the width of the integrand in the vicinity of k^* . As a result, the second derivative of Ψ satisfies

$$\Psi''(\theta) \simeq \int_0^\infty \frac{k(k-1)}{\theta^2} p(k) \theta^k dk \simeq \frac{k_0(k_0-1)}{\theta^2} \Psi(\theta), \quad (36)$$

where the slowly-varying prefactors were taken out of the integral and evaluated at $k^* \simeq k_0$. This allows solving Eq. (25) for the leading-order of S_{opt} , by plugging Eq. (36) into (25). Here, we still have an unknown prefactor of θ^{-2} , but it turns out that for the sake of its calculation, it suffices to take $p_k = \delta_{k,k_0}$ which yields $\theta \sim \Psi^{1/k_0}$. Hence, in the leading order in $k_0 \gg 1$ we find

$$\Psi(\theta_{\text{opt}}^{(0)}) \simeq \frac{1}{R_0} \left(1 + \epsilon^2 + \frac{1 + R_0 - 2 \ln R_0}{k_0}\right). \quad (37)$$

Here, we have kept $\mathcal{O}(\epsilon^2)$ terms but neglected $\mathcal{O}(\epsilon^2/k_0)$ terms. This result is completely generic for any distribution with a mean degree of k_0 and coefficient of variation ϵ , as long as $\epsilon \ll 1$. Plugging Eq. (37) into (34) we have found the optimal fraction of susceptibles at the onset of quarantine which minimizes R_∞ for generic networks.

Notably, while the estimation of the HDI threshold (i.e., solving $\dot{I} = 0$) can only be done numerically in the case of generic heterogeneous networks, Eq. (37) provides an approximate analytic expression for this threshold for generic networks with a narrow degree distribution. We show this numerically in the following section.

III. RESULTS

We now present results for S_{opt} —the optimal fraction of susceptibles at the onset of quarantine that minimizes R_{∞} . We do so for the various networks we have studied, and check our theoretical predictions for S_{opt} (27) by using two numerical methods: (i) solving the deterministic rate equations and (ii) performing network-based simulations. Notably, through this validation of the theoretical results, we aim to gain a deeper understanding of the optimal quarantine strategies across different networks.

The first numerical method includes solving the deterministic rate equations, in which at time $t = t_0$, a temporary quarantine is initiated for a duration of Δt . We do so over a wide range of S_b values and determine the final outbreak fraction R_{∞} for each case. By fitting a parabolic curve to the function $R_{\infty}(S_b)$, we identify the optimal S_b that minimizes R_{∞} .

The second numerical method includes performing network-based simulations. For this, we have constructed networks that follow the prescribed degree distributions using the configurational model, which gives rise to networks with negligible degree-degree correlations [43]. In this work we have focused on four different types of networks: well-mixed, homogeneous, Poisson and gamma networks. Nevertheless, the formalism is generic and we can simulate any arbitrary network (including empirical networks) with a given degree distribution. For each network, we have used the Gillespie algorithm [44–46] and ran Monte Carlo (MC) simulations for each S_b value. As done with the rate equations, we identified the optimal S_b by determining which value minimizes R_{∞} .

We have already established the existence of an optimal S_b in Fig. 2 for two different networks, by showing heatmaps of R_{∞} versus S_b , while varying both R_0 and Δt . In Fig. 3, we compare our theoretical predictions for S_{opt} with a numerical solution of the rate equations and MC simulations, for well-mixed and Poisson networks. Here we show the dependence of S_{opt} on the quarantine’s strength, ξ . The agreement between the theoretical and numerical results is excellent. The dashed horizontal line indicates the HDI threshold which is approached as $\xi \rightarrow 0$. The HDI threshold equals $1/R_0$ for a well-mixed topology, and is calculated numerically for the Poisson network. Our results indicate that as the system approaches the HDI threshold, the number of infected individuals should increase at the onset of an optimal quarantine. Consequently, more stringent quarantine measures (lower ξ) are required to effectively minimize the overall expected outbreak size.

In Fig. 4 we wanted to check our conjecture that as the quarantine duration decreases, S_{opt} approached the HDI threshold S_{hdi} in the absence of quarantine. To this end, we plotted the relative difference $(S_{\text{opt}} - S_{\text{hdi}})/S_{\text{opt}}$ as a function of R_0 and quarantine duration Δt , for Poisson and gamma networks. Indeed, as $\Delta t \rightarrow 0$, the relative distance vanishes. Also, as expected, the relative distance changes at a steeper rate as R_0 is increased, see Fig. 4.

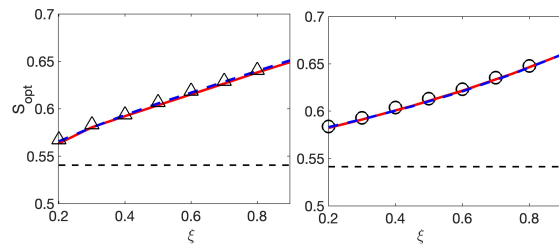


FIG. 3. Optimal fraction of susceptibles, S_{opt} , versus ξ for $R_0 = 1.85$ and quarantine duration $\Delta t = 2$. Left and right panels show results for a well-mixed and Poisson network, respectively, with $k_0 = 80$. In both panels a numerical solution of the rate equations (solid lines) is compared to the theoretical prediction [Eqs. (13) and (31)] (dashed lines) and MC simulations (triangles and circles). Horizontal dashed line marks the HDI threshold in the absence of a quarantine.

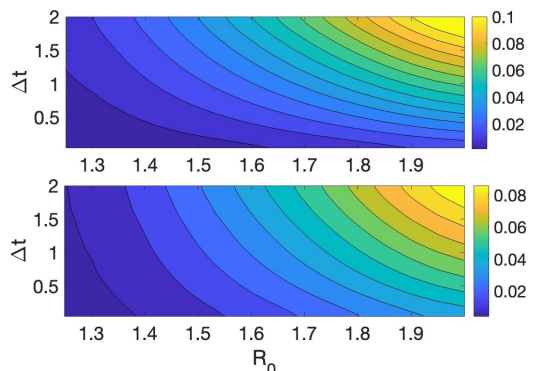


FIG. 4. Heatmaps of the relative distance between S_{opt} and the HDI threshold, for a Poisson (upper panel) and gamma (lower panel) network, versus R_0 and Δt . Warmer (cooler) colors indicate larger (smaller) relative distances. Here $k_0 = 20$, $\xi = 0.5$, and $\epsilon = 0.45$ (in the lower panel).

In Fig. 5 we have studied the dependence of S_{opt} on the average degree k_0 , in the case of homogeneous, Poisson, and gamma networks. The figure shows that S_{opt} increases as the mean degree decreases. Importantly, this indicates that as the network is more connected (with an increasing number of edges), the quarantine measures should be initiated at a later stage. Naturally, the reason is that by varying k_0 , we effectively vary the critical infection rate below which the infection wave dies out instantly. As k_0 is decreased, β_c is increased, see Eq. (14), which means that by keeping R_0 constant, we effectively increase the infection rate. This means that the quarantine should start at an earlier stage, with less infected individuals. In the inset, we plot S_{opt} as function of k_0 but vary R_0 in such a way that R_{∞} in the absence of quarantine remains the same. In this case, as seen in the inset S_{opt} remains almost constant, as the effect of increasing k_0 is balanced by decreasing R_0 .

In Fig. 6 we further probe our conjecture that S_{opt} coincides with the HDI threshold as the quarantine duration Δt goes to zero. To this end, we plot the difference between S_{opt} and S_{hdi} as function of Δt , for a large variety of networks with varying k_0 and ϵ .

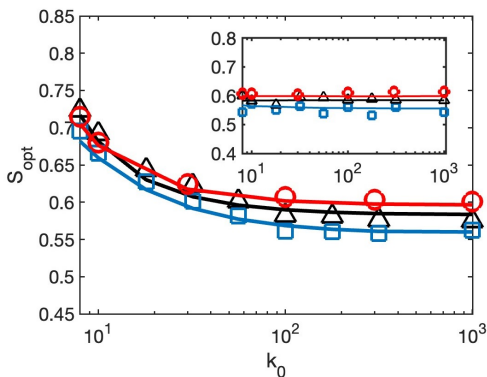


FIG. 5. Shown is S_{opt} versus k_0 for $R_0 = 1.85$, $\xi = 0.4$ and quarantine duration $\Delta t = 2$. Here we compare the numerical solution of the rate equations (solid lines) and MC simulation (symbols), for three different networks: homogeneous (triangles), Poisson (squares), and gamma (circles). For the latter we took a coefficient of variation of $\epsilon = 0.25$. Inset shows the same comparison, but here R_0 varies with k_0 such that R_∞ in the absence of quarantine remains unchanged.

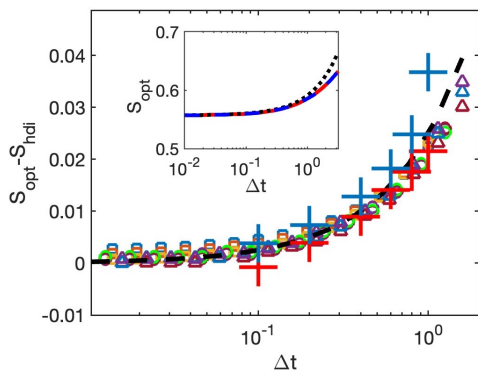


FIG. 6. The difference $S_{\text{opt}} - S_{\text{hdi}}$ versus Δt , computed by numerically solving the rate equations, for homogeneous (triangles) and Poisson (squares) networks with $k_0 = 50, 100, 1000$, and for gamma networks (circles) with $k_0 = 50$ and $\epsilon = 0.01, 0.05, 1$. For all networks $R_0 = 1.7$. Plus symbols are MC simulations for a Poisson (blue) and gamma (red) network, with $k_0 = 80$ and $\epsilon = 0.25$ for the latter. Dashed line represents the theoretical prediction (34). Inset shows S_{opt} versus Δt , comparing between the numerical solution of the rate equations (solid line), semi-analytical prediction (dashed line) and approximated theoretical prediction (dotted line), in a Poisson network with $k_0 = 50$, $\xi = 0.5$, and $R_0 = 1.9$.

Figure 6 shows two important features. First, it proves that as $\Delta t \rightarrow 0$, S_{opt} approaches S_{hdi} , and that $S_{\text{hdi}} \simeq \Psi(\theta_{\text{opt}}^{(0)})$, see Eqs. (34) and (37). Although the HDI threshold cannot be computed analytically for arbitrary networks, our results strongly support the fact that the analytical expression in Eq. (37) is an excellent approximation for S_{hdi} . Second, the figure shows that the universal first-order correction in $\Delta t \ll 1$ that we have found for any arbitrary network, excellently agrees with

numerical solutions of the deterministic rate equations and numerical MC simulations for a wide variety of network topologies. In the inset we show a comparison between the approximated theoretical prediction [Eq. (31)], valid for short Δt and large k_0 , the semi-analytical prediction, found by numerically solving Eq. (21) during the quarantine for $\Delta\theta(S_b)$, and the full numerical solution of the rate equations. One can see that the theoretical approximation remains accurate as long as $\Delta t \ll 1$.

IV. DISCUSSION AND CONCLUSION

We have studied the optimal timing for initiating temporary quarantine measures within the SIR model on heterogeneous networks, in order to reduce epidemic impact. By analyzing how the quarantine timing impacts the epidemic curve, we were able to determine the initiation point that would most effectively limit the spread, i.e., the fraction of susceptibles at the start of quarantine.

Our theoretical framework was based on the mean-field, deterministic theory, and we computed the optimal susceptible fraction S_{opt} at the onset of the quarantine, which minimizes the final outbreak fraction, R_∞ . Our results were obtained for four prototypical network structures: well-mixed (fully connected), homogeneous, Poisson and gamma networks. Importantly, when the quarantine duration is not too long, we have derived analytical expressions for the optimal timing of the quarantine, also for generic networks with an arbitrary (narrow) degree distribution. Our results reveal that in this case, the optimal moment to begin quarantine occurs just before the herd immunity (HDI) threshold is reached. This finding is counterintuitive, as naïvely one would think early intervention is more efficient. However, initiating quarantine too early may only delay the epidemic's peak rather than reduce its size, as it prevents sufficient immunity accumulation. We have also shown that for highly connected networks quarantine measures should be initiated at a later stage compared with sparse networks.

Our conclusions emphasize the importance of well-timed quarantine measures in effectively managing epidemics. Interventions aligned with the HDI threshold enable a balance between delaying the epidemic and promoting the development of natural immunity, ultimately minimizing the total expected outbreak size.

Future directions include incorporating stochastic effects such as demographic noise into the model to capture the variability and unpredictability of real-life epidemics with a finite population. Furthermore, exploring ways to determine the HDI threshold directly from timing the optimal quarantine may become a practical tool for epidemic control in networked populations, potentially aiding in more responsive public health decision-making.

- [1] R. M. Anderson and R. M. May, *Infectious diseases of humans: dynamics and control* (Oxford university press, 1991).
- [2] W. O. Kermack and A. G. McKendrick, A contribution to the mathematical theory of epidemics, Proceedings of the royal society of london. Series A, Containing papers of a mathematical and physical character **115**, 700 (1927).
- [3] D. Mollison, *Epidemic models: their structure and relation to data*, 5 (Cambridge University Press, 1995).
- [4] D. J. Daley and J. M. Gani, *Epidemic modelling: an introduction*, 15 (Cambridge University Press, 1999).
- [5] H. W. Hethcote, The mathematics of infectious diseases, SIAM review **42**, 599 (2000).
- [6] M. J. Keeling and K. T. Eames, Networks and epidemic models, Journal of the royal society interface **2**, 295 (2005).
- [7] L. J. Allen, An introduction to stochastic epidemic models, in *Mathematical epidemiology* (Springer, 2008) pp. 81–130.
- [8] H. Andersson and T. Britton, *Stochastic epidemic models and their statistical analysis*, Vol. 151 (Springer Science & Business Media, 2012).
- [9] W. Yang, D. Zhang, L. Peng, C. Zhuge, and L. Hong, Rational evaluation of various epidemic models based on the covid-19 data of china, Epidemics **37**, 100501 (2021).
- [10] J. Hindes, M. Assaf, and I. B. Schwartz, Outbreak size distribution in stochastic epidemic models, Physical Review Letters **128**, 078301 (2022).
- [11] R. Pastor-Satorras, C. Castellano, P. Van Mieghem, and A. Vespignani, Epidemic processes in complex networks, Reviews of modern physics **87**, 925 (2015).
- [12] M. Saeedian, M. Khalighi, N. Azimi-Tafreshi, G. Jafari, and M. Ausloos, Memory effects on epidemic evolution: The susceptible-infected-recovered epidemic model, Physical Review E **95**, 022409 (2017).
- [13] M. Bohner, S. Streipert, and D. F. Torres, Exact solution to a dynamic sir model, Nonlinear Analysis: Hybrid Systems **32**, 228 (2019).
- [14] M. J. Keeling, The effects of local spatial structure on epidemiological invasions, Proceedings of the Royal Society of London. Series B: Biological Sciences **266**, 859 (1999).
- [15] A.-L. Barabási and R. Albert, Emergence of scaling in random networks, science **286**, 509 (1999).
- [16] R. Pastor-Satorras and A. Vespignani, Epidemic spreading in scale-free networks, Physical review letters **86**, 3200 (2001).
- [17] C. Moore and M. E. Newman, Epidemics and percolation in small-world networks, Physical Review E **61**, 5678 (2000).
- [18] M. E. Newman, Assortative mixing in networks, Physical review letters **89**, 208701 (2002).
- [19] J. Hindes and M. Assaf, Degree dispersion increases the rate of rare events in population networks, Physical review letters **123**, 068301 (2019).
- [20] P. Erdős and A. Rényi, On random graphs, Publ. Math. **6**, 290 (1959).
- [21] H. C. Thom, A note on the gamma distribution, Monthly weather review **86**, 117 (1958).
- [22] L. A. Adamic, R. M. Lukose, A. R. Puniyani, and B. A. Huberman, Search in power-law networks, Physical review E **64**, 046135 (2001).
- [23] J. Neipel, J. Bauermann, S. Bo, T. Harmon, and F. Jülicher, Power-law population heterogeneity governs epidemic waves, PloS one **15**, e0239678 (2020).
- [24] F. Ball, A unified approach to the distribution of total size and total area under the trajectory of infectives in epidemic models, Advances in Applied Probability **18**, 289 (1986).
- [25] F. Ball and D. Clancy, The final size and severity of a generalised stochastic multitype epidemic model, Advances in applied probability **25**, 721 (1993).
- [26] M. J. Keeling and P. Rohani, *Modeling infectious diseases in humans and animals* (Princeton university press, 2011).
- [27] T. House, J. V. Ross, and D. Sirl, How big is an outbreak likely to be? methods for epidemic final-size calculation, Proceedings of the Royal Society A: Mathematical, Physical and Engineering Sciences **469**, 20120436 (2013).
- [28] L. J. Allen, A primer on stochastic epidemic models: Formulation, numerical simulation, and analysis, Infectious Disease Modelling **2**, 128 (2017).
- [29] J. C. Miller, Distribution of outbreak sizes for sir disease in finite populations, arXiv preprint arXiv:1907.05138 (2019).
- [30] J. Hindes, L. Mier-y Teran-Romero, I. B. Schwartz, and M. Assaf, Outbreak-size distributions under fluctuating rates, Physical Review Research **5**, 043264 (2023).
- [31] M. E. Newman, Spread of epidemic disease on networks, Physical review E **66**, 016128 (2002).
- [32] L. A. Meyers, B. Pourbohloul, M. E. Newman, D. M. Skowronski, and R. C. Brunham, Network theory and sars: predicting outbreak diversity, Journal of theoretical biology **232**, 71 (2005).
- [33] E. Kenah and J. M. Robins, Second look at the spread of epidemics on networks, Physical Review E—Statistical, Nonlinear, and Soft Matter Physics **76**, 036113 (2007).
- [34] E. Volz, Sir dynamics in random networks with heterogeneous connectivity, Journal of mathematical biology **56**, 293 (2008).
- [35] J. C. Miller, A note on a paper by erik volz: Sir dynamics in random networks, Journal of mathematical biology **62**, 349 (2011).
- [36] D. Meidan, N. Schulmann, R. Cohen, S. Haber, E. Yaniv, R. Sarid, and B. Barzel, Alternating quarantine for sustainable epidemic mitigation, Nature communications **12**, 220 (2021).
- [37] X. Yan, Y. Zou, and J. Li, Optimal quarantine and isolation strategies in epidemics control, World Journal of Modelling and Simulation **3**, 202 (2007).
- [38] J. Hindes, S. Bianco, and I. B. Schwartz, Optimal periodic closure for minimizing risk in emerging disease outbreaks, PLoS One **16**, e0244706 (2021).
- [39] Going back to physical time units, this requirement means that that the quarantine duration is much shorter than the typical time for recovery.
- [40] A. H. Nayfeh, *Perturbation methods* (John Wiley & Sons, 2008).
- [41] S. Morita, Basic reproduction number of epidemic models on sparse networks, Physical Review E **106**, 034318 (2022).
- [42] A. Leibenzon and M. Assaf, Heterogeneity can markedly

- increase final outbreak size in the sir model of epidemics, *Physical Review Research* **6**, L012010 (2024).
- [43] B. K. Fosdick, D. B. Larremore, J. Nishimura, and J. Ugander, Configuring random graph models with fixed degree sequences, *Siam Review* **60**, 315 (2018).
- [44] D. T. Gillespie, A general method for numerically simulating the stochastic time evolution of coupled chemical reactions, *Journal of computational physics* **22**, 403 (1976).
- [45] D. T. Gillespie, Exact stochastic simulation of coupled chemical reactions, *The journal of physical chemistry* **81**, 2340 (1977).
- [46] D. T. Gillespie, Stochastic simulation of chemical kinetics, *Annu. Rev. Phys. Chem.* **58**, 35 (2007).